

FULL PAPER

Design and synthesis of hydrazinecarbothioamide sulfones as potential antihyperglycemic agents

Ashraf A. Aly¹  | Alaa A. Hassan¹ | Maysa M. Makhlouf¹ |
 Mohammed B. Alshammari² | Sara Mohamed Naguib Abdel Hafez³ |
 Marwa M. M. Refaie⁴  | Stefan Bräse^{5,6}  | Martin Nieger⁷ | Mohamed Ramadan⁸ 

¹Department of Chemistry, Faculty of Science, Minia University, El-Minia, Egypt

²Prince Sattam bin Abdulaziz Department of Chemistry, College of Sciences and Humanities, Alkharj, Saudi Arabia

³Department of Histology and Cell Biology, Faculty of Medicine, Minia University, El-Minia, Egypt

⁴Department of Pharmacology, Faculty of Medicine, Minia University, El-Minia, Egypt

⁵Institute of Organic Chemistry, Karlsruhe Institute of Technology, Karlsruhe, Germany

⁶Institute of Biological and Chemical Systems, Karlsruhe Institute of Technology, Hermann-von-Helmholtz-Platz 1, Eggenstein-Leopoldshafen, Germany

⁷Department of Chemistry, University of Helsinki, Helsinki 00014, Helsinki, A. I. Virtasen aukio 1, Finland

⁸Department of Pharmaceutical Organic Chemistry, Faculty Pharmacy, Al-Azahr University, Assiut Branch, Assiut, Egypt

Correspondence

Ashraf A. Aly, Department of Chemistry, Faculty of Science, Minia University, El-Minia 61511, Egypt.
 Email: ashrafaly63@yahoo.com and ashraf.shehata@minia.edu.eg

Abstract

New hydrazinecarbothioamides with a phenylsulfonyl group were synthesized and their structures were identified by different spectroscopic data (¹H NMR, ¹³C NMR, two-dimensional NMR, mass spectrometry, elemental analysis, and single-crystal X-ray analysis). The mechanism describing the formation of the products was also discussed. The antidiabetic activity of the isolated products was investigated histochemically. The synthesized sulfonylalkylthiosemicarbazide exhibited antihyperglycemic activity in streptozotocin-induced diabetic mice. Compounds **5a** and **5c** significantly lowered the blood glucose level to 103.3 ± 1.8 and 102 ± 3.9 mg/dl, respectively. Also, they caused a significant decrease in malondialdehyde levels and normalized the glutathione levels in streptozotocin-induced diabetic mice, compared with the diabetic group. The results suggest that the synthesized hydrazinecarbothioamides may effectively inhibit the development of oxidative stress in diabetes.

KEYWORDS

4-substituted hydrazinecarbothioamides, antihyperglycemic activity, bis(2-(phenylsulfonyl)ethyl)sulfane, glutathione, malondialdehyde, sulfonylalkylthiosemicarbazide

1 | INTRODUCTION

Due to the significant impact of sulfone compounds in biological applications, the development of new sulfone-containing compounds remains one of the central challenges of organic chemistry.^[1,2] There are many sulfones widely reported in the literature with a broad spectrum of biological activities such as anticancer,^[3] antimicrobial,^[4] anti-inflammatory,^[5] antiproliferative,^[6,7] antimalarial^[8] and anti-HIV activities.^[9] Catalytic chemoselective addition of amino alcohols to α,β-unsaturated sulfonyl derivatives leads to the regioselective formation of amino and hydroxy adducts, depending on different catalysts and

reaction conditions.^[10,11] N-Substituted hydrazinecarbothioamides are considered as one of the most important classes of compounds containing nitrogen, sulfur, and oxygen used for heterocyclization and formation of different heterocyclic rings such as thiadiazole and thiadiazepine, and from the reaction with several π-deficient compounds.^[12–15] The literature approach was applied to 4-(1-phenyl-1H-tetrazole-5-ylsulfonyl)butanenitrile (PTSB), a growth inhibitory compound with a previously unknown mode of action, and the thioredoxin/thioredoxin reductase system was identified as its target.^[16] Another patent showed compounds having CH₂CH₂SO₂Ar functional group as histone deacetylase inhibitors.^[17–18] The synthesis of various heterocyclic

rings, for example, pyrazoles, triazole thione, and thiadiazoles, can be obtained via reaction of *N*-substituted hydrazinecarbothioamides with both 2-bis(methylthio)methylene)malononitrile and ethyl 2-cyano-3,3-bis(methylthio)acrylate.^[19] In light of our general aim to screen compounds of biological and pharmaceutical importance, we designed, synthesized, and screened a large variety of biologically active compounds.^[20-27]

The total number of people with diabetes has been projected to increase from 171 million in 2000 to 366 million by 2030. Diabetes mellitus (DM) is managed by insulin and oral administration of hypoglycemic drugs such as sulfonylureas and biguanides.^[28] DM is divided into three main types: type I, type II, and gestational diabetes. Type II diabetes mellitus (T2DM) accounts for more than 90% of all diabetic cases.^[29] T2DM is a heterogeneous disease associated with both genetic and environmental causative factors including multiple defects in insulin secretion and action.^[30,31] Insulin is a hormone that moves glucose inside the cells to produce energy. Upon inadequate insulin secretion, the glucose level in the blood increases (hyperglycemia). An extended period of hyperglycemia causes irreversible damage to the eyes, kidneys, nerves, and heart.^[32] Hyperglycemia can be controlled by the administration of insulin, which suppresses glucose production and augments glucose utilization. Major classes of drugs used in the treatment of DM are insulins, sulfonylureas, thiazolidinediones, biguanides, meglitinides, α -glucosidase inhibitors, dipeptidyl peptidase-4 inhibitors, glucagon-like peptide-1 agonists, sodium-glucose cotransporter 2 inhibitors, and dopamine agonists.^[33] Sulfonylurea agents act by increasing insulin from β islet cells, whereas biguanides act by reducing the excessive hepatic glucose production. Tolbutamide (**1**, Figure 1) was the first-generation sulphonylurea drug developed, which was later surpassed by the second-generation gliclazide, glipizide, and glibenclamide (glyburide), and the third-generation agent glimepiride (**2**, Figure 1).^[34] However, these agents are associated with severe and sometimes fatal hypoglycemia, gastric disturbances like nausea, vomiting, heartburn, anorexia, and increased appetite.^[35,36] Nevertheless, these hypoglycemic agents are actively pursued, as it is very difficult to maintain normoglycemia by any means in patients with DM. Therefore, the discovery of new hypoglycemic scaffolds with minimum side effects is still a challenge to medicinal chemists.^[37-39]

It is also perceived that in the case of diabetes, an increase of reactive oxides and peroxides of lipids occurs along with the lower activity of antioxidative factors.^[40-44] The mechanism that is responsible for the

development of oxidative stress in diabetes has not been univocally determined. A factor probably of greatest significance is hyperglycemia occurring with hypoinsulinemia.^[45] The lack of insulin leads to insulin-dependent disturbances in glucose metabolism, which is accompanied by an increase in the autooxidation of glucose. During this process, the reduction of the oxygen molecule and the generation of free radicals occur. Insulin substitution causes a decrease in lipid peroxidation, an increase in the activity of antioxidative systems, and normalization of glucose levels.^[45,46]

Although many examples of sulfonyl(thio)ureas are known, there has been a limited investigation concerning separation by an alkyl linker. However, a recent patent (US 2013-14108597) offers a first insight into the successful combination for the treatment of DM.

In this study, we disclose the reactivity of *N*-substituted hydrazinecarbothioamides **3a-d** toward active sulfonyl compound, (vinylsulfonyl)benzene (**4**) via the Michael addition reaction. The nucleophilic addition between **3a-d** and **4** affords different Michael adducts, depending on various active sites on hydrazinecarbothioamides. Most indicative is to design compounds having a combination of two structures, with both being bioactive scaffolds; one contains the PhSO₂CH₂CH₂ moiety and the other contains variable RNHCSNHNH groups as bioactive scaffolds (Figure 2). The application of sulfonylalkylthiosemicarbazide as antihyperglycemic agents is not common. Herein, we report a facile way for the preparation of sulfonylalkylthiosemicarbazides and we test and screen their antihyperglycemic activity using streptozotocin-induced diabetic mice, blood glucose level, and antioxidative enzyme activity. Also, a histological study of the pancreas is performed, compared with glimepiride.

2 | RESULTS AND DISCUSSION

2.1 | Chemistry

An equimolar mixture of hydrazinecarbothioamides **3a-d** and (vinylsulfonyl)benzene (**4**) was refluxed in absolute ethanol containing catalytic amount of triethylamine, Et₃N (0.5 ml), for 3–4 h, which afforded *N*-substituted-2-(2-(phenylsulfonyl)ethyl)hydrazinecarbothioamides **5a-d**, *N*2,*N*5-diphenyl-1,3,4-thiadiazole-2,5-diamine (**6a**), and bis(2-(phenylsulfonyl)ethyl)sulfane (**7**) (Scheme 1). The reaction conditions

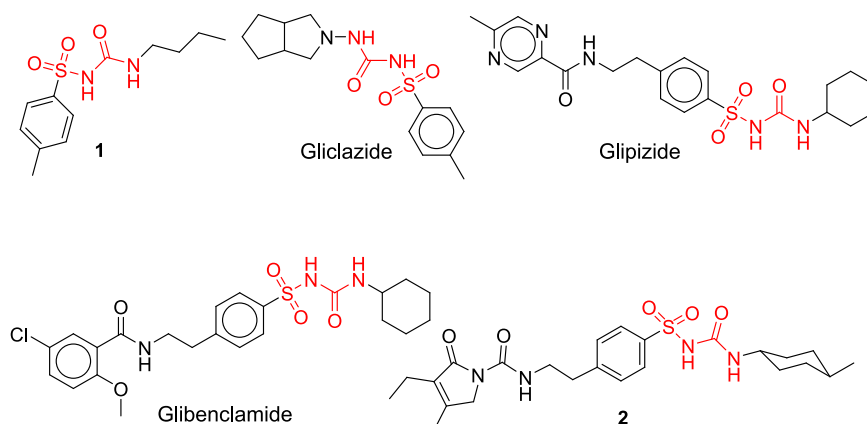


FIGURE 1 Chemical structures of some sulfonylurea drugs

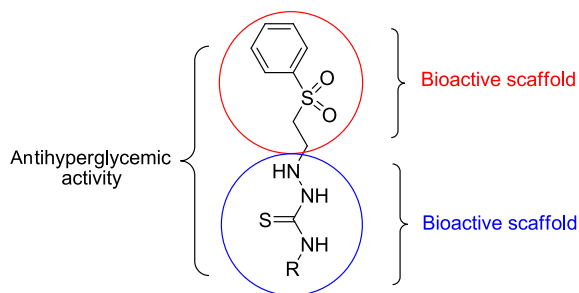


FIGURE 2 Design of the target compounds **5a-d**

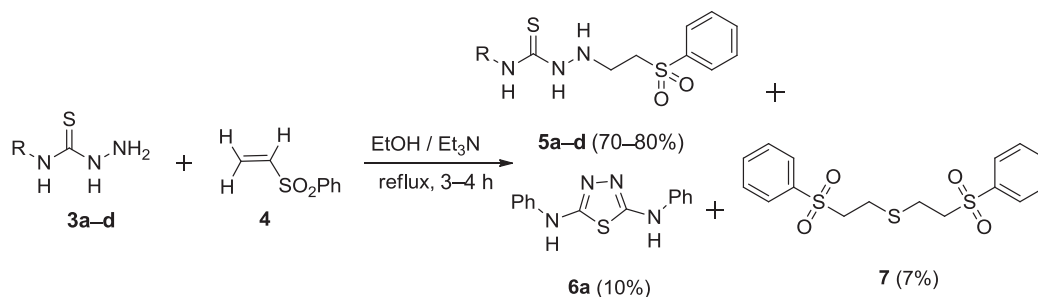
(i.e., temperature, solvent, and/or catalyst) play an important role in the reaction efficiency and product obtained; thus, different temperatures and solvents such as dimethylformamide, ethyl acetate (EtOAc), and tetrahydrofuran were used. Also, the use of catalytic amounts with few drops of triethylamine or piperidine as inexpensive catalysts at room temperature or refluxing temperature resulted in low yields and impure products. However, the use of absolute ethanol and a few drops of triethylamine while refluxing was the most efficient condition to get high yields.

The nucleophilic addition of *N*-substituted hydrazinecarbothioamides **3a-d** to vinylsulfonyl-benzene (**4**) gave *N*-substituted-2-(2-(phenylsulfonyl)ethyl)hydrazinecarbothioamides **5a-d** instead of the expected cyclized product (*Z*)-*N*-(5-(phenylsulfonyl)-1,3,4-thiadiazinan-2-ylidene)-substituted amines **9a-d**, which would be obtained via intermediate **8a-d** (Scheme 2).

The formation of the products **6a** and **7** may be discussed via tautomerism between thione and thiol of **3a-d**, which was followed by the formation of the salt **A**. Elimination of a molecule of hydrazine from **A** would form an isothiocyanate intermediate (Scheme 3). Nucleophilic attack of the hydrazinyl-*N* lone pair of **3a** on thiocarbonyl of isothiocyanate intermediate would give **B**, and then another nucleophilic attack of thione lone pair on the thiocarbonyl carbon would give **C**. *N*²,*N*⁵-Diphenyl-1,3,4-thiadiazol-2,5-diamine (**6a**)^[47] was obtained via eliminating H₂S molecule

from compound **12**. Finally, bis(2-(phenylsulfonyl)ethyl)sulfane **7**^[48] was obtained via reaction of (vinylsulfonyl)benzene (**4**) with H₂S. It is well known that all the conjugate additions with vinyl sulfones share a similar reaction pattern by addition at the β -position of the sulfone. Hence, these reactions are a well-established method of creating β -heterosubstituted sulfones. In all cases, the resulting 1,4-addition products contain either the sulfonyl moiety, which can undergo subsequent functional group transformations or can be easily removed, making these compounds a perfect choice to afford easily naked alkyls.^[49] Therefore, the extruded H₂S would add to **4** to give the zwitter ion **D** (Scheme 3), which would be neutralized into the thiol compound **E**. The addition of **E** to another molecule of **4** would form **7** (Scheme 3). The structures of compounds **6a** and **7** were confirmed via single-crystal X-ray structure analyses (Figures 3 and 4).

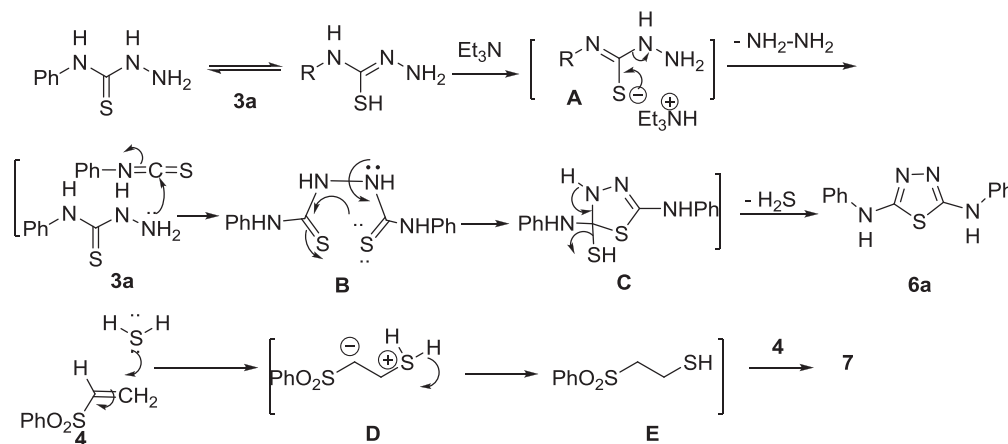
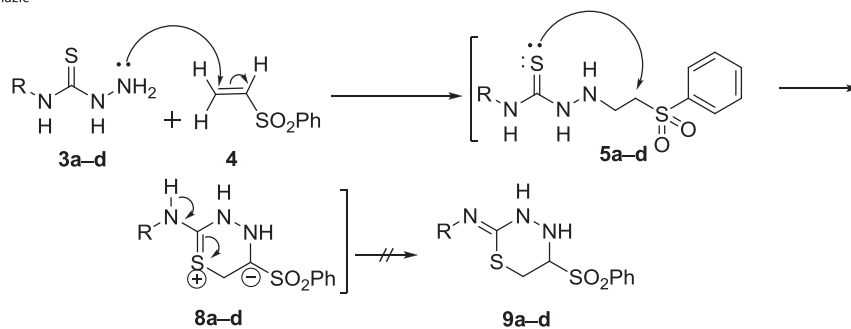
The molecular structure of the obtained compounds **5a-d** was confirmed on the basis of their mass spectrometric, infrared (IR), ¹H NMR (nuclear magnetic resonance), ¹³C NMR, two-dimensional (2D) NMR data (Section 4). As an example, the structure of compound **5b** (Figure 5) and its NMR spectroscopic data showed that H-1a is distinctive at $\delta_{\text{H}} = 4.02$; its attached carbon appears at $\delta_{\text{C}} = 51.66$. H-1a gives COSY correlation with NH-1, with the 2H signal at $\delta_{\text{H}} = 1.82$ and with the 4H signal at $\delta_{\text{H}} = 1.25$. Each of these proton signals gives heteronuclear single quantum correlation (HSQC) with carbon at $\delta_{\text{C}} = 32.08$. The signal at $\delta_{\text{H}} = 1.82$ is assigned as one pair of the nonequivalent H-1b, 2H signal at $\delta_{\text{H}} = 1.25$ is assigned as the other pair of H-1b, and the carbon at $\delta_{\text{C}} = 32.08$ is assigned as C-1b. The other 2H signal at $\delta_{\text{H}} = 1.25$ and the 2H signal at $\delta_{\text{H}} = 1.68$ are assigned as the two pairs of H-1c; their attached carbon appears at $\delta_{\text{C}} = 24.68$. The 1H signals at $\delta_{\text{H}} = 1.57$ and 1.12 are assigned as the nonequivalent H-1d; their attached carbon appears at $\delta_{\text{C}} = 25.11$ ppm. Besides, in the case of compound **5d** (Figure 5) as an example, the IR spectrum showed absorptions at $\nu = 3318, 3200, 3050, 2973, 1362, \text{ and } 1592 \text{ cm}^{-1}$ due to NHs, Ar-CH, Ali-CH, C=S, and Ar-C=C, respectively. NMR spectroscopic data showed a 3H triplet in ¹H NMR at $\delta_{\text{H}} = 1.05$, assigned as H-1b, and the attached carbon appears at $\delta_{\text{C}} = 14.58$. H-1b gives COSY correlation and



Substrate	5a	5b	5c	5d
R	Phenyl	Cyclohexyl	Allyl	Ethyl
Yield (%)	80	75	73	70

SCHEME 1 The reaction between *N*-substituted hydrazinecarbothioamides **3a-d** and (vinylsulfonyl)benzene **4**

SCHEME 2 The Michael addition of *N*-substituted hydrazinecarbothioamides **3a–d** to (vinylsulfonyl)benzene **4**



SCHEME 3 The mechanism for the formation of compounds **6a** and **7**

C-1b gives heteronuclear multiple bond correlation (HMBC), with the downfield part of the 4H envelope between $\delta_H = 3.44$ and 3.42 , assigned as H-1a; this envelope gives HSQC with carbon at $\delta_C = 37.68$, which also gives HMBC with H-1b, so this carbon is assigned as C-1a (Figure 5). H-1b gives HMBC with nitrogen (N-1) at $\delta_N = 115.3$, N-1 gives HSQC with its attached proton at $\delta_H = 7.89$, and HMBC with another NH proton at $\delta_H = 8.76$, assigned as N-3. N-3 gives HSQC with its attached nitrogen at $\delta_N = 134.6$ and HMBC with the 2H “quartet” (H-4a) at $\delta_H = 2.92$. H-4a gives HMBC with carbon at $\delta_C = 180.64$, assigned as C-2, and with the upfield half of the envelope between $\delta_H = 3.44$ and 3.42 , assigned as H-4b. The phenyl signals are assigned straightforwardly (Section 4). Elemental analysis and mass spectrometry confirmed the formation of Michael adduct from the presence of molecular ion peak at 287 [M^+ , 100], corresponding to the molecular formula of $C_{11}H_{17}N_3O_2S_2$.

2.2 | Biology

2.2.1 | Oxidative stress parameters (malondialdehyde [MDA] and reduced glutathione [GSH]) and blood glucose

The results with the new compound **5** showed a significant decrease in MDA and blood glucose in all treated groups, compared with the diabetic group. Moreover, GSH was significantly normalized in

these groups as compared with the diabetic group. However, MDA, GSH, and blood glucose significantly increased in the diabetic group as compared with the control group (Table 1).

2.2.2 | Hematoxylin and eosin stain (H&E) results

Pancreatic sections from the control group showed a normal lobular structure. The pancreatic tissue showed both pancreatic acini and islets of Langerhans. The pancreatic acini appeared with basal basophilia and apical acidophilia. The islet of Langerhans, pale areas between acini, showed cells with vesicular nuclei and intercellular blood vessels. Regarding the diabetic group, massive lobular distortion and dilated blood vessels were noticed. Most of the pancreatic acini displayed dense nucleoli. Other acini showed apoptotic nuclei.

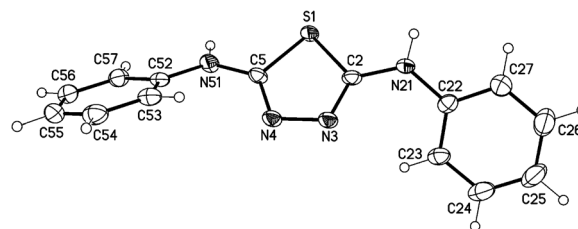


FIGURE 3 The molecular structure of compound **6a** (displacement parameters are drawn at 50% probability level)

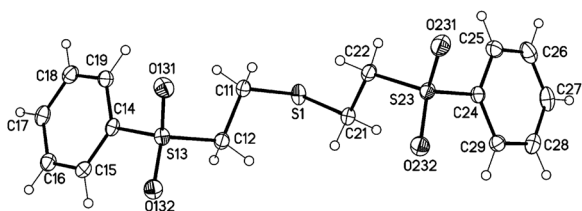


FIGURE 4 The molecular structure of compound 7 (displacement parameters are drawn at 50% probability level)

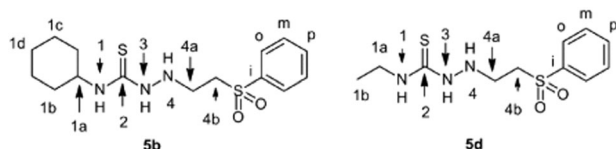


FIGURE 5 The distinctive structures of compounds 5b and 5d

Degenerated islets of Langerhans and the inflammatory cell infiltration were frequently detected (Figures 6 and 7).

In the current work, diabetes resulted in severe distortion of the islets with an apparent decrease in their cellularity. These findings were in agreement with those of previous researchers^[50] who revealed the presence of shrunken islets with hydropic degeneration of the cytoplasm in the diabetic pancreas. It was reported that the damaging effects of DM on islet β cells were mediated *via* the inhibition of free radical scavenger enzyme, resulting in activation of the production of superoxide, which is implicated in lipid oxidation, DNA damage, and sulfhydryl oxidation, leading to degranulation and loss of capacity to secrete insulin.^[51]

Also, there was a marked degeneration of the pancreatic acini with loss of its basal basophilic and apical acidophilic portions. The mechanism of degeneration of the exocrine parenchyma in DM was attributed to the loss of high levels of insulin that perfuse the acini, resulting in a trophic effect.^[52] Both 5b and 5d showed amelioration of lobular architecture. The islet of Langerhans appeared with more numerous vesicular cells. Most pancreatic acini restored their basal basophilic and apical acidophilic portions. 5a and 5c exhibited more or less normal pancreatic tissue and normal pancreatic architecture, and almost all pancreatic acini appeared with basal basophilia and apical acidophilia. In most sections, invisible dilated blood vessels were observed (Figures 6 and 7).

2.2.3 | Morphometric analysis

There was a highly significant decrease in the mean diameter of islets in the diabetic group if compared with the control one. However, there was a significant increase in this parameter in 5a and 5d if compared with the diabetic groups. Additionally, there was a low significance difference between drugs 5a and 5c if compared with drugs 5b and 5d (Figure 8).

2.3 | Molecular docking

The K_{ATP} channels in pancreatic β cells indirectly sense blood glucose concentration and gate insulin release. When blood glucose concentration is elevated, the ATP concentration inside β cells also increases due to the active glucose uptake and metabolism. ATP can directly bind and inhibit K_{ATP} , thereby leading to the depolarization of β cell plasma membrane and activation of voltage-gated calcium channels. Calcium influx triggers insulin release from β cells.^[53] The closure of pancreatic K_{ATP} channels is integral to insulin secretion, and sulfonylureas, which inhibit K_{ATP} channels, are widely used to treat type II diabetes. To rationalize the remarkable effect of the synthesized analogs, molecular modeling and visualization processes were carried out with the referred site of pancreatic ATP-sensitive potassium channel obtained from the Protein Data Bank (PDB code: 5WUA) using Molecular Operating Environment (MOE®) version 2014.09. In this study, we docked all derivatives, 5a–d, and glimepiride, as a reference, to predict the binding interactions between the newly synthesized hydrazinecarbothioamide sulfones and this site that is known to be involved in ligand binding and enzymatic catalysis. The theoretical predictions from the molecular docking study were found to agree with some highly active derivatives such as 5b and 5d with the antihyperglycemic activity. All derivatives were successfully docked, and the binding free energies from the major docked poses are listed in Table 2 and the most favorable 2D poses of the tested compounds are shown in (Figure 9). Scoring function (S score) is used to approximately predict the binding affinity between ligand and protein receptor. Most of the tested compounds have a high binding affinity to the enzyme, as their binding free energy (ΔG) values range from -0.6 to -2.4 kcal/mol, comparable to the reference glimepiride ($\Delta G = -0.8$ to -1.4 kcal/mol).

The docking result of the reference compound glimepiride is completely consistent with the mode of action of hydrazinecarbothioamide sulfones derivatives 5a–d. Stabilization of the reference compound glimepiride within the active site occurred through two hydrogen bond

TABLE 1 Oxidative stress parameters MDA, GSH, and blood glucose

Groups	Blood glucose (mg/dl)	MDA (nmol/g tissue)	GSH (mmol/g tissue)
Control	95 ± 2.9	1.212 ± 0.039	0.433 ± 0.033
5a	103.3 ± 1.8 ^a	10.440 ± 0.273 ^{ab}	0.633 ± 0.033 ^{ab}
5b	256.7 ± 8.8 ^{ab}	3.750 ± 0.303 ^{ab}	0.567 ± 0.033 ^a
5c	102.3 ± 3.9 ^a	3.038 ± 0.404 ^{ab}	0.633 ± 0.033 ^{ab}
5d	195 ± 19 ^{ab}	1.552 ± 0.0189 ^a	0.600 ± 0.010 ^{ab}
Glimepiride	101.1 ± 2.9 ^{ab}	3.394 ± 0.314 ^{ab}	0.725 ± 0.022 ^{ab}
Diabetic	520 ± 15 ^b	30.640 ± 0.254 ^b	3.167 ± 0.033 ^b

Note: Values are a representation of observations as means ± SEM. Results are considered significantly different when $p < .05$.

Abbreviations: GSH, reduced glutathione; MDA, malondialdehyde.

^aSignificant difference compared with the diabetic group.

^bSignificant difference compared with control.

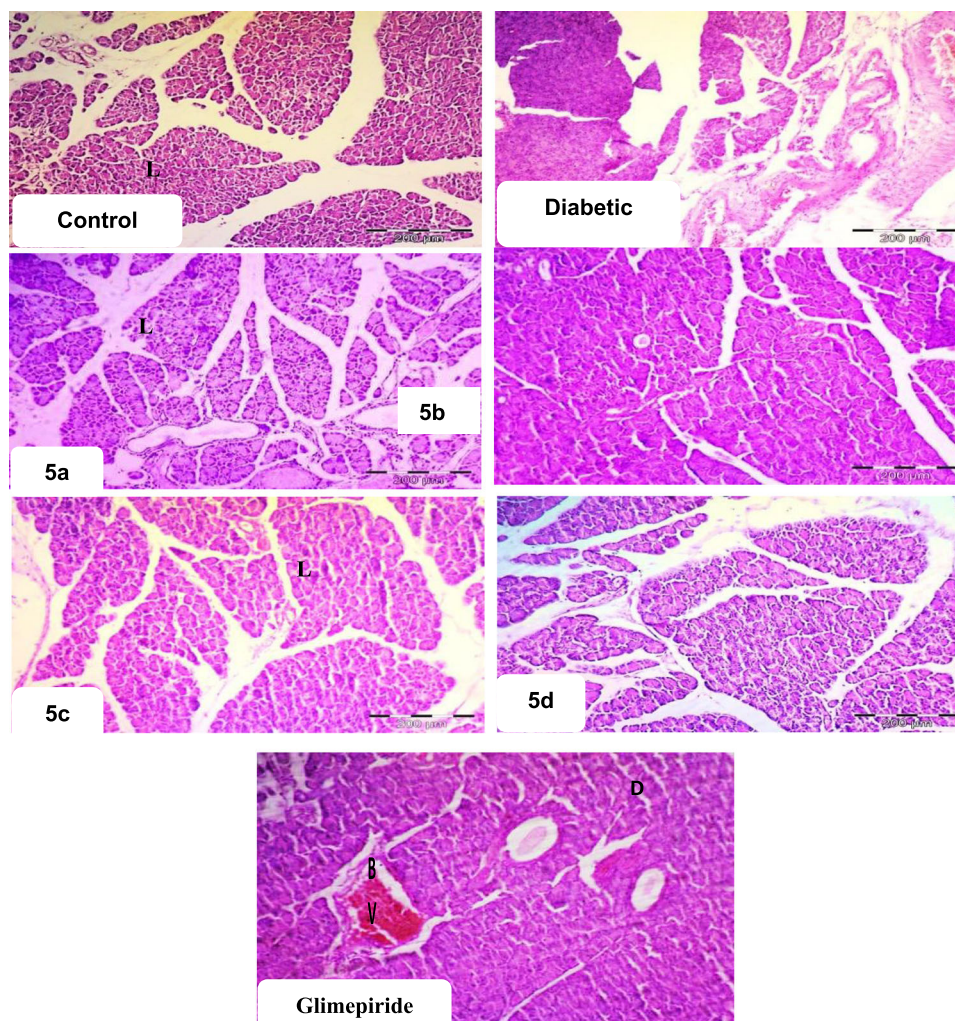


FIGURE 6 Photomicrographs of pancreatic sections revealed the control pancreatic tissue showing a normal lobular structure (L). The diabetic group showed a marked lobular distortion (D) and dilated blood vessels (BV). **5b** and **5d** showed amelioration of lobular architecture (L) with less dilated BV and amelioration of lobular architecture. **5a** and **5c** showed more or less normal pancreatic tissue (hematoxylin and eosin stain $\times 100$)

interactions with amino acid residue Phe 1496 (Figure 9). Docking results with pancreatic K_{ATP} channel enzyme revealed that most of the tested compounds show good binding and form several interactions, comparable to that of the reference compound glimepiride. Compound **5a** (Figure 9) exhibited two H-bonding interactions with Pro 1429 and hydrophobic interaction with Leu 1431. Moreover, compound **5b** showed two hydrogen bonds with Ala 1493 and Arg 1494, and two hydrophobic bonds with Ile 1457 and Ala 1527 (Figure 9). However, compound **5c** (Figure 9) formed two hydrogen bonds with the amino acid residues Thr 1450 and Arg 1494. Compound **5d** formed two hydrogen bonds with Arg 1494 and Tyr 512 (Figure 9).

2.4 | Structure–activity relationship

From the biological results and docking studies, it was concluded that sulfonylalkylthiosemicarbazide could be introduced as a new class of

antidiabetic agents with sulfonylurea-like activity. The essential moieties for activity are the thiosemicarbazide and phenylsulfonyl. In addition, the extra N atom in thiosemicarbazide offers an additional site for H-bond formation with the protein that improves fitting, compared with sulfonylureas. Moreover, the separation between phenylsulfonyl and thiosemicarbazide moieties with ethyl group did not reduce activity. The effect of the thiosemicarbazide substituents R (phenyl, cyclohexyl, allyl, and ethyl) on the activity is not significant.

3 | CONCLUSION

New hydrazinocarbothioamides derivatives were synthesized in a simple chemical reaction, and the synthesized hydrazinocarbothioamides were screened for their antihyperglycemic activity in streptozotocin-induced diabetic mice. Results showed a significant decrease in MDA

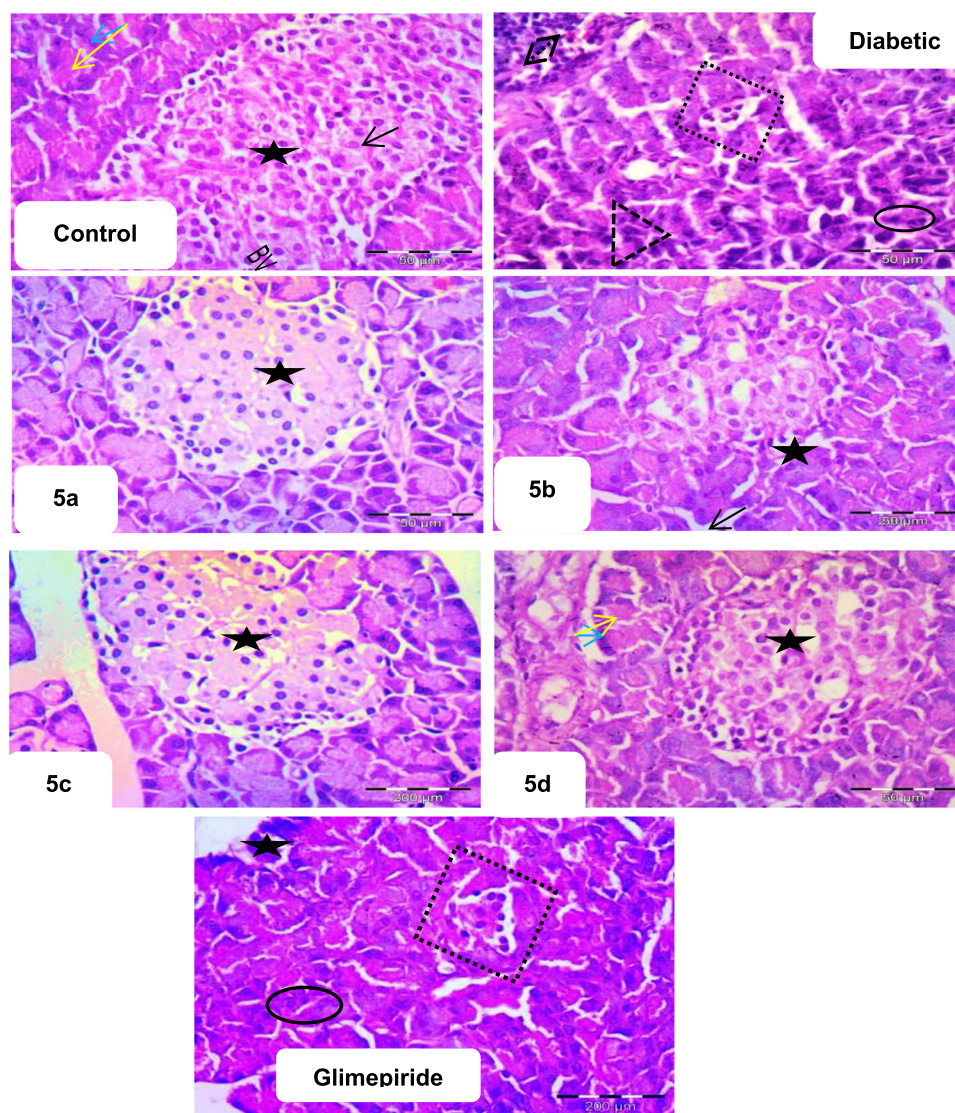


FIGURE 7 Photomicrographs of pancreatic sections revealed the control pancreatic tissue showing islet of Langerhans (star) with vesicular cells (arrow) and intercellular blood vessels. The pancreatic acini appeared with basal basophilia (blue arrow) and apical acidophilia (yellow arrow). The diabetic group showed degenerated islet of Langerhans (rectangle) and the inflammatory cell infiltration (double arrow). The pancreatic acini appeared with dense nucleoli (triangle). Others showed apoptotic nuclei (circle). **5b** and **5d** showed amelioration of acinar architecture. Islet of Langerhans appeared with more numerous vesicular cells (star). Most acini restored their basal basophilia (blue arrow) and apical acidophilia (yellow arrow). **5a** and **5c** showed more or less normal pancreatic tissue. Glimepiride showed islet of Langerhans appearing with more cells than the previous group (square). Still, some acini exhibited with apoptotic cells (circle) and others showed degenerated acini (star) (hematoxylin and eosin stain $\times 400$)

and blood glucose in all treated groups, compared with the diabetic group. Moreover, GSH significantly increased in these groups, compared with the diabetic group. The results confirmed by histopathological studies revealed the ability of the synthesized compounds to protect pancreatic cells from massive lobular distortion, dilated blood vessels, degenerated islets of Langerhans, and the inflammatory cell infiltration noticed in the diabetic group. Compounds **5a** and **5c** revealed the most significant reduction in blood glucose, which reflects the importance of the presence of an efficient π system in the side chain of hydrazinocarbothioamides.

4 | EXPERIMENTAL

4.1 | Chemistry

4.1.1 | General

Melting points (MPs) were recorded on a Gallenkamp melting point apparatus (Gallenkamp) by using open capillaries and were uncorrected. NMR data were recorded on a Bruker AM 400 spectrophotometer, $^1\text{H-NMR}$ (400 MHz), and $^{13}\text{C-NMR}$ (100 MHz). Chemical shifts were

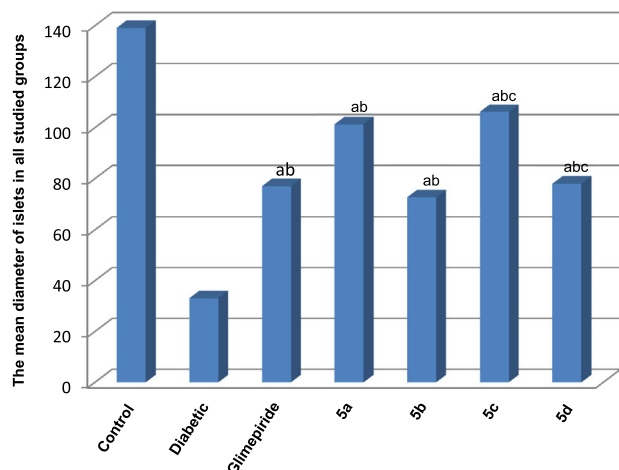


FIGURE 8 All studied groups showed the mean diameter of islets in ps. Results represent the mean \pm SEM ($n = 6$). ^aSignificant difference from the control group, ^bsignificant difference from the diabetic group, and ^csignificant difference from 5a ($p < 0.05$)

reported in ppm from tetramethylsilane using solvent resonance in CDCl_3 or deuterated dimethyl sulfoxide ($\text{DMSO}-d_6$) solutions as the internal standard; s = singlet, t = triplet, q = quartet, m = multiplet, br = broad. The ^{13}C -NMR signals were assigned on the basis of DEPT 135/90 spectra. The mass spectra were obtained on a Finnigan MAT 312 instrument using electron impact ionization (70 eV). The IR spectra were recorded on a Bruker Alpha FT-IR instrument with samples prepared as potassium bromide pellets. Thin-layer chromatography (TLC) was performed on precoated plates (silica gel 60 PF₂₅₄), and zones were

TABLE 2 Energy scores for the complexes formed by the tested compounds 5a–d and the reference glimepiride in the active site of pancreatic K_{ATP} channels (PDB: 5WUA)

Compound	S score	ΔG (kcal/mol) ^a	Ligand–receptor interaction		
			Residue	Type	Length (Å)
Glimepiride	-7.38	-1.4	Phe 1496	H-donor	3.36
			Phe 1496	H-acceptor	3.10
5a	-6.10	-1.5	Pro 1429	H-donor	3.17
			Pro 1429	H-donor	3.05
			Leu 1431	Pi–H	3.99
5b	-6.01	-0.9	Ala 1493	H-donor	2.76
			Arg 1494	H-acceptor	3.94
			Ile 1457	Pi–H	3.95
			Ala 1527	Pi–H	4.00
5c	-5.63	-0.9	Thr 1450	H-donor	3.13
			Arg 1494	H-acceptor	4.01
5d	-5.56	-0.8	Arg 1494	H-donor	3.00
			Tyr 512	H-donor	4.16

^aThe binding free energies.

visualized with ultraviolet light. Elemental analyses for C, H, and N were carried out with Elementar 306.

The InChI codes of the investigated compounds, together with some biological activity data, are provided as Supporting Information.

4.1.2 | Synthesis of compounds 3a–d

N-Substituted hydrazinecarbothioamides 3a–d were prepared according to literature procedures (3a,^[54]3b,^[55]3c,^[56] and 3d^[57]). Also, phenylvinyl sulfone 4 was purchased from Fluka.

4.1.3 | Reaction of *N*-substituted hydrazinecarbothioamides 3a–d and phenylvinyl sulfone (4)

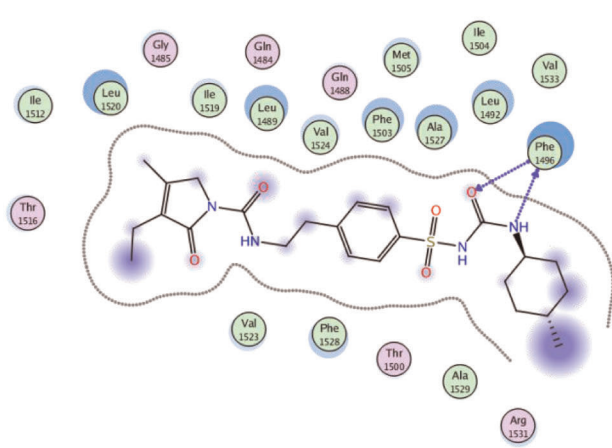
The *N*-substituted-2-[2-(phenylsulfonyl)ethyl]hydrazinecarbothioamides 5a–d were synthesized via refluxing different solutions of the *N*-substituted hydrazinecarbothioamides 3a–d (1 mmol) and 4 in dry EtOH containing 0.5 ml of triethylamine for 3–4 h. The reaction was monitored by TLC, showing the total consumption of the starting materials. The resulting mixtures were subjected to PLC (plate layer chromatography) where two zones are separated using toluene/EtOAc (10:5) as an eluent. The slowest zone contained 5a–d, whereas compound 7 was obtained as the highest zone for all substituents of 3a–d. Also, in the case of 3a, another product 6a was obtained as colorless crystals during recrystallization from ethanol.

N-Phenyl-2-[2-(phenylsulfonyl)ethyl]hydrazinecarbothioamide (5a)

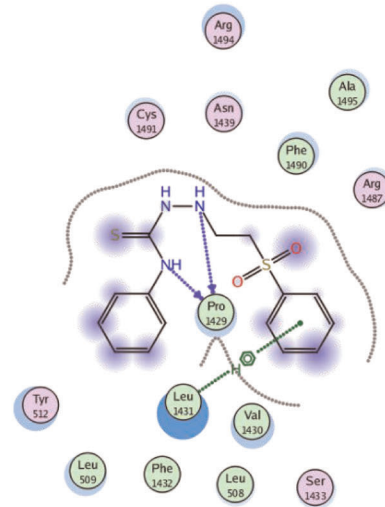
Yield: 0.268 g (80%); colorless crystals (EtOH); MP: 87–88°C. IR (KBr): $\nu = 3300, 3246$ (NHs), 3105 (Ar-H), 2922 (Ali-CH), 1368 (C=S), and 1593 (Ar-C=C) cm^{-1} . ^1H NMR (400 MHz, $\text{DMSO}-d_6$): $\delta = 2.95$ (q, 2H, CH_2 , $J = 6.6$), 3.40 (m, 2H, CH_2N), 5.05 (s, 1H, ^4NH), 7.06 (m, 3H, Ar-H), 7.32 (m, 3H, Ar-H), 7.71 (m, 2H, Ar-H), 7.82 (m, 2H, Ar-H), 8.01 (s, 1H, ^1NH), and 9.10 ppm (s, 1H, ^3NH). ^{13}C NMR (100 MHz, $\text{DMSO}-d_6$): $\delta = 47.31$ (CH_2N), 56.00 ($\text{CH}_2\text{-SO}_2$), 125.3, 126.72, 128.17, 129.50, 131.00, 133.22 (Ar-CH), 139.26, 139.66 (Ar-C), and 181.00 (C=S) ppm. MS: m/z (70 eV, %) = 335 [M^+ , 51], 194 (10), 155 (30), 154 (100), 136 (72), 107 (21), and 77 (17). Anal. calcd. for $\text{C}_{15}\text{H}_{17}\text{N}_3\text{O}_2\text{S}_2$ (335.44); C, 53.71; H, 5.11; N, 12.53; S, 19.12. Found: C, 53.77; H, 5.19; N, 12.45; S, 19.22.

N-Cyclohexyl-2-[2-(phenylsulfonyl)ethyl]hydrazinecarbothioamide (5b)

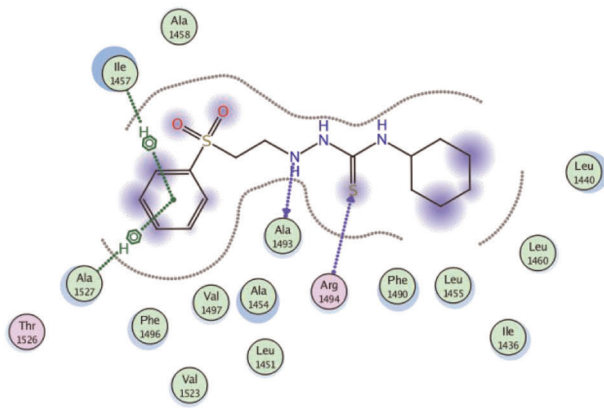
Yield: 0.256 g (75%); colorless crystals (EtOH); MP: 171–172°C. IR (KBr): $\nu = 3320, 3250$ (NHs), 3077 (Ar-H), 2940 (Ali-CH), 1368 (C=S), and 1593 (Ar-C=C) cm^{-1} . NMR ($\text{DMSO}-d_6$): 1.12 (bt, $J = 10$ Hz, 1H, H-1d), 1.25 (m, 4H, H-1b,1c), 1.57 (bd, $J = 12$ Hz; 1H, H-1d), 1.68 (m, 2H, H-1c), 1.82 (m, 2H, H-1b), 2.93 (dt, $J_d = 5.0$; $J_t = 6.6$ Hz; 2H, H-4a), 3.39 (t, $J = 6.7$; 2H, H-4b), 4.02 (m, 1H, H-1a), 5.12 (t, $J = 4.1$ Hz; 1H, H-4), 7.69 (s, 1H, NH-1), 7.70 (t, $J = 7.6$ Hz; 2H, H-m),



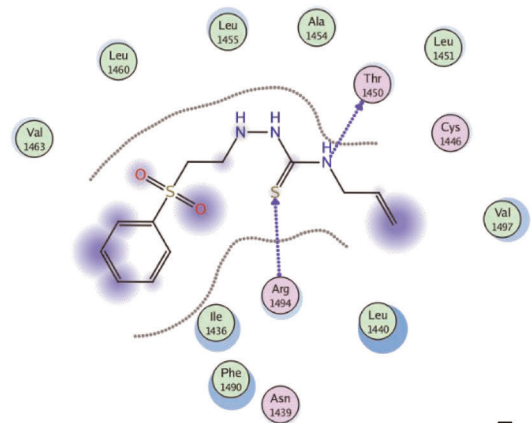
Glimepiride



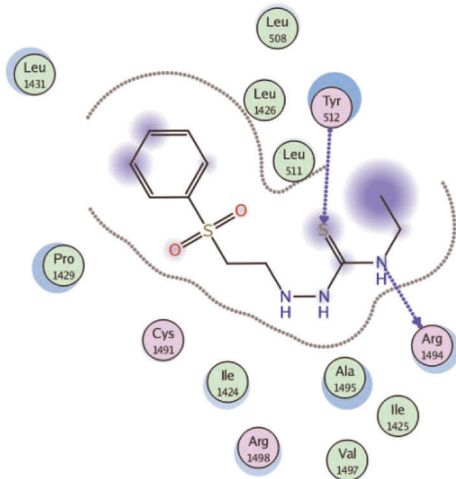
5a



5b



5c



5d

FIGURE 9 Two-dimensional diagrams illustrating the binding modes of the reference glimepiride and 5a-d interaction with the active site of pancreatic K_{ATP} channels

7.79 (tt, $J = 7.4, 1.5$ Hz; 1H, H-p), 7.90 (dd, $J = 7.2; 1.4$ Hz; 2H, H-o), and 8.75 (s; 1H, NH-3). ^{13}C NMR (100 MHz, DMSO- d_6): $\delta = 24.68, 25.11, 32.08, 44.18, 51.66, 52.91, 127.79, 129.57, 133.96, 139.09, \text{ and } 179.71$. ^{15}N NMR (40 MHz, DMSO- d_6): $\delta = 69.5, 125.7, \text{ and } 134.6$ ppm. MS: m/z (70 eV, %) = 341 [M^+ , 100], 200 (17), 185 (11), 154 (31), and 115 (45). Anal. calcd. for $\text{C}_{15}\text{H}_{23}\text{N}_3\text{O}_2\text{S}_2$ (341.49): C, 52.76; H, 6.79; N, 12.30; S, 18.78. Found: C, 52.69; H, 6.84; N, 12.23; S, 18.82.

N-Allyl-2-[2-(phenylsulfonyl)ethyl]hydrazinecarbothioamide (5c)

Yield: 0.218 g (73%); colorless crystals (EtOH); MP: 82–83°C. IR (KBr): $\nu = 3355, 3294$ (NHs), 3100 (Ar-H), 2919 (Ali-CH), 1350 (C=S), and 1596 (Ar-C=C) cm^{-1} . ^1H NMR (400 MHz, DMSO- d_6): $\delta = 2.93$ (q, 2H, $J = 6.5$ Hz; CH_2), 3.42 (m, 2H, $\text{CH}_2\text{-SO}_2$), 4.08 (m, 2H, CH_2N), 5.09 (m, 2H, $\text{CH}_2\text{=CH}$), 5.81 (m, 1H, $\text{CH}_2\text{=CH}$), 5.13 (s, 1H, ^4NH), 7.69 (t, 2H, $J = 7.5$ Hz; Ar-H), 7.78 (t, 1H, $J = 7.3$ Hz; Ar-H), 7.96 (s, 1H, ^1NH), 7.88 (d, 2H, $J = 7.6$ Hz; Ar-H), and 8.83 ppm (s, 1H, ^3NH). ^{13}C NMR (100 MHz, DMSO- d_6): $\delta = 45.35$ (CH_2N), 44.24 ($\text{CH}_2\text{-allyl}$), 53.12 ($\text{CH}_2\text{-SO}_2$), 115.35 ($\text{CH}_2\text{=CH}$), 127.52, 129.57, 134.00 (Ar-CH), 135.18 ($\text{CH}_2\text{=CH}$), 139.04 (Ar-C), and 180.73 (C=S) ppm. MS: m/z (70 eV, %) = 299 [M^+ , 100], 200 (17), 185 (11), 154 (31), and 115 (45). Anal. calcd. for $\text{C}_{12}\text{H}_{17}\text{N}_3\text{O}_2\text{S}_2$ (299.41): C, 48.09; H, 5.67; N, 14.03; S, 21.37. Found: C, 48.16; H, 5.75; N, 13.96; S, 21.30.

N-Ethyl-2-[2-(phenylsulfonyl)ethyl]hydrazinecarbothioamide (5d)

Yield: 0.209 g (70%); colorless crystals (EtOH); MP: 148–149°C. IR (KBr): $\nu = 3318, 3200$ (NHs), 3050 (Ar-H), 2973 (Ali-CH), 1362 (C=S), and 1592 (Ar-C=C) cm^{-1} . ^1H NMR (400 MHz, DMSO- d_6): $\delta = 1.05$ (t, $J = 7.0$ Hz; 3H, H-1b), 2.92 (q, $J = 6.4$ Hz; 2H, H-4a), 3.42 (m; 2H, H-4b), 3.44 (m; 2H, H-1a), 5.08 (s; 1H, H-4), 7.70 (t, $J = 7.4$ Hz; 1H, H-m), 7.79 (t, $J = 7.2$ Hz; 1H, H-p), 7.89 (s; 1H, NH-1), 7.90 (d, $J = 7.6$ Hz; 2H, H-o), and 8.76 (s; 1H, NH-3). ^{13}C NMR (100 MHz, DMSO- d_6): $\delta = 14.58, 37.68, 44.25, 53.10, 127.55, 129.59, 133.99, 139.05, \text{ and } 180.64$. ^{15}N NMR (40 MHz, DMSO- d_6): $\delta = 70.0, 115.3, \text{ and } 134.6$ ppm. MS: m/z (70 eV, %) = 287 [M^+ , 100], 257 (13), 200 (25), 185 (10), 146 (9), and 103 (6). Anal. calcd. for $\text{C}_{11}\text{H}_{17}\text{N}_3\text{O}_2\text{S}_2$ (287.40): C, 45.92; H, 5.91; N, 14.61; S, 22.26. Found: C, 46.01; H, 5.99; N, 14.69; S, 22.33.

N2,N5-Diphenyl-1,3,4-thiadiazole-2,5-diamine (6a)

Yield: 0.026 g (10%); colorless crystals.^[58]

Bis[2-(phenylsulfonyl)ethyl]sulfane (7)

Yield: 0.019 g (7%); colorless crystals (EtOH); MP: 120–121°C [lit. MP: 115–116°C].^[41] ^{13}C NMR (101 MHz, DMSO- d_6): $\delta = 23.86$ (CH_2), 54.64 (CH_2), 127.73, 129.44, 133.86 (Ar-CH), and 138.73 (Ar-C).

4.1.4 | Single-crystal X-ray structure determination of 6a and 7

Single crystals of **6a** and **7** were obtained by recrystallization from EtOH. The single-crystal X-ray structure analyses were carried out

on a Bruker D8 Venture diffractometer with a Photon II CPAD detector at 123 K using Cu-K α radiation ($\lambda = 1.54178$ Å). Dual-Space Methods (SHELXT)^[59] for **6a** and **7** were used for structure solution and refinement was carried out using SHELXL-2014 (full-matrix least-squares on F^2)^[60] for **6a** and **7**. Hydrogen atoms were refined using a riding model (H [N] free). Semiempirical absorption corrections were applied.

CCDC 1886120 (**6a**, M. Nieger, A. A. Aly, S. Bräse, CSD Communication, 2018) and CCDC 1968395 (**7**) contain the Supporting Information Crystallographic Data for this paper. These data can be obtained free of charge from The Cambridge Crystallographic Data Centre via www.ccdc.cam.ac.uk/data_request/cif.

Compound 6a

$\text{C}_{14}\text{H}_{12}\text{N}_4\text{S}$, Mr = 268.34 g mol^{-1} , yellow crystals, size $0.16 \times 0.16 \times 0.04$ mm, monoclinic, space group Pc (no. 7), $a = 11.0926$ (5) Å, $b = 7.0662$ (3) Å, $c = 8.5212$ (4) Å, $\beta = 104.429$ (2) Å, $V = 646.85$ (5) Å 3 , $Z = 2$, $D_{\text{calcd}} = 1.378$ Mg m^{-3} , $F(000) = 280$, $\mu = 2.14$ mm^{-1} , $T = 123$ K, 8154 measured reflections ($2\theta_{\text{max}} = 144.2^\circ$), 2397 independent reflections ($R_{\text{int}} = 0.024$), 178 parameters, 4 restraints, R_1 (for $2362 > 2\sigma$ [I]) = 0.033, wR^2 (for all data) = 0.087, $S = 1.05$, largest diff. peak and hole = $0.30 \text{ e } \text{Å}^{-3} / -0.18 \text{ e } \text{Å}^{-3}$. The absolute structure was determined by the refinement of Flack's x -parameter $x = -0.01(2)$.^[61] Compound **6a** is a redetermination of HAHGUT/HAHGUT01 (CSD refcode) at 123 K using Cu-K α radiation. For HAHGUT, see CCDC-237483 at lit.^[62] and for HAHGUT01, see CCDC-1020639, please see lit.^[63]

Compound 7

$\text{C}_{16}\text{H}_{18}\text{O}_4\text{S}_3$, Mr = 370.48 g mol^{-1} , colorless crystals, size $0.16 \times 0.06 \times 0.02$ mm, monoclinic, space group $\text{P}2_1/c$ (no. 14), $a = 12.1183$ (3) Å, $b = 5.2041$ (1) Å, $c = 26.5839$ (7) Å, $\beta = 101.814$ (1) Å, $V = 1641.00$ (7) Å 3 , $Z = 4$, $D_{\text{calcd}} = 1.500$ Mg m^{-3} , $F(000) = 776$, $\mu = 4.28$ mm^{-1} , $T = 123$ K, 15,972 measured reflections ($2\theta_{\text{max}} = 144.2^\circ$), 3233 independent reflections ($R_{\text{int}} = 0.033$), 208 parameters, R_1 (for $2954 > 2\sigma$ [I]) = 0.036, wR^2 (for all data) = 0.091, $S = 1.10$, largest diff. peak and hole = $0.50 \text{ e } \text{Å}^{-3} / -0.46 \text{ e } \text{Å}^{-3}$.

4.2 | Pharmacological/biological assays

4.2.1 | Animal experiments, ethical approval

Minia University Faculty of Medicine Research Ethics Committee “BFMREC” approved this study proposal regarding the source of the animals, health status, inclusion criteria, exclusion criteria, caging, comfort, and the detailed experimental design and procedures. It was conducted in agreement with the NIH Guide for Care and Use of Laboratory Animals.

Adult male Wistar albino rats weighing about 250–300 g were purchased from the Animal Research Centre, Giza, Egypt. Rats were left in standard housing conditions (three rats/cage) and were left to acclimatize for 1 week. Animals were supplied with laboratory chow and tap water. Rats were randomly divided into seven groups ($n = 6$ each).

1. Control group rats were given an intraperitoneal injection of 0.5 ml/kg citrate buffer saline as a vehicle twice weekly for 14 days.
2. Diabetic group: Rats received a single intraperitoneal injection of 50 mg/kg STZ for induction of diabetes,^[64] the other five groups were treated with compounds **5a-d** and glimipride as a reference drug.
3. After 14 days, each rat was weighed and then killed. Venous blood was collected from the jugular vein and centrifuged at 5000 rpm for 15 min (JanetzkiT30 centrifuge). After sacrifice, the pancreas was excised and weighed. Parts of the pancreas was taken then fixed in 10% formalin and embedded in paraffin for histopathological examinations. The remaining parts were snap-frozen in liquid nitrogen and kept at -80°C . Pancreatic tissue homogenates were prepared for biochemical analysis (Glas-Col homogenizer). Pancreas homogenate was centrifuged at 3000 rpm for 20 min and the supernatant was kept at -80°C until used.

4.2.2 | Evaluation of pancreatic tissue MDA and reduced GSH^[65]

MDA was detected depending on a reaction with the thiobarbituric acid. The colored complexes were evaluated spectrophotometrically at 535 nm and calculated using the standard curve of 1,1,3,3-tetramethoxypropane.^[66] The GSH determination method was based on the reduction of Ellman's reagent by the thiol groups of GSH to produce a yellow color, which was measured spectrophotometrically at 412 nm.^[67]

4.2.3 | Histopathology study

Fresh small pieces of pancreatic tissue were obtained from each rat and rapidly fixed in 10% neutral-buffered formalin, dehydrated in a graded alcohol series, cleared with xylene, and embedded in paraffin wax. Sections (5 μm thick) were stained with H&E for studying the general histological structure.^[68]

4.2.4 | Photography

An Olympus (U.TV0.5XC-3) light microscope and digital camera were used in this current study. Images were performed using Adobe Photoshop.

4.2.5 | Morphometric study

The mean diameter of the islets of Langerhans was measured in this study. Measurement of the average islet core diameter and exclusion of the extension areas were carried out. This was performed using power $\times 400$ from 10 successive nonoverlapping fields.^[69]

4.2.6 | Statistical analysis

Results were expressed as means \pm standard error of the mean.^[70] One-way analysis of variance, followed by the Tukey-Kramer post-analysis test, was used to analyze the results, and p values less than 0.05 were considered significant. GraphPad Prism was used for statistical calculations (version 3.02 for Windows, GraphPad Software, www.graphpad.com).

4.3 | Molecular docking

A docking simulation study was performed using the Molecular Operating Environment (MOE®) version 2014.09, Chemical Computing Group Inc. The target compounds were constructed into a 3D model using the builder interface of the MOE program. After checking their structures and the formal charges on atoms by the 2D depiction, the following steps were carried out:

1. All conformers were subjected to energy minimization; all the minimizations were performed with MOE until a root mean square deviation (RMSD) gradient of 0.01 kcal/mol and RMS distance of 0.1 Å with MMFF94X force field, and the partial charges were automatically calculated.
2. The obtained data base was then saved as a Molecular Data Base (MDB) file to be used in the docking calculations.

4.3.1 | Optimization of the target

The X-ray crystallographic structure of the target K_{ATP} channel (PDB: 5WUA) was obtained from the Protein Data Bank. The compounds were docked on the active site of the target enzyme.

The enzyme was prepared for docking studies by the following methodology:

1. The cocrystallized ligand was deleted.
2. Hydrogen atoms were added to the system with their standard geometry.
3. The atoms' connection and type were checked for any errors with automatic corrections.
4. The selection of the receptor and its atoms potential were fixed.

4.3.2 | Docking of the target molecules to K_{ATP} channel active site

Docking of the target compounds was done using MOE-Dock software. The following methodology was generally applied:

The enzyme active site file was loaded and the Dock tool was initiated. The program specifications were adjusted to the following:

- Dummy atoms as the docking site.

- Triangle matcher as the placement methodology to be used.
- London dG as scoring methodology to be used, which was adjusted to its default values.

1. The MDB file of the ligand to be docked was loaded, and Dock calculations were run automatically.
2. The obtained poses were studied, and the poses that showed the best ligand–enzyme interactions were selected and stored for energy calculations.

ACKNOWLEDGMENT

The authors thank the DFG Foundation for providing a 2-month fellowship to Prof. Ashraf A. Aly, enabling him to carry out the analysis of the compounds in the Karlsruhe Institute of Technology, Karlsruhe, Germany, in July–August 2019.

ORCID

Ashraf A. Aly  <https://orcid.org/0000-0002-0314-3408>

Marwa M. M. Refaie  <http://orcid.org/0000-0001-6211-9558>

Stefan Bräse  <https://orcid.org/0000-0003-4845-3191>

Mohamed Ramadan  <https://orcid.org/0000-0002-7975-3421>

REFERENCES

- [1] H.-B. Yang, A. Feceu, D. B. C. Martin, *ACS Catal.* **2019**, *9*, 5708. <https://doi.org/10.1021/acscatal.9b01394>
- [2] I. Ahmad, Shagufta, *Int. J. Pharm. Pharm. Sci.* **2015**, *7*, 19.
- [3] M. S. Al-Said, M. M. Ghorab, Y. M. Nissan, *Chem. Cent. J.* **2012**, *6*, 64. <https://doi.org/10.1186/1752-153X-6-64>
- [4] N. Ahmed, N. K. Konduru, M. Owais, *Arabian J. Chem.* **2019**, *12*, 1879. <https://doi.org/10.1016/j.arabjc.2014.12.008>
- [5] B. Tozkoparan, E. Küpeli, E. Yeşilada, M. Ertan, *Bioorg. Med. Chem.* **2007**, *15*, 1808. <https://doi.org/10.1016/j.bmc.2006.11.029>
- [6] A. Cohen, M. D. Crozet, P. Rathelot, N. Azas, P. Vanelle, *Molecules* **2013**, *18*, 97. <https://doi.org/10.3390/molecules18010097>
- [7] A. R. Usera, P. Dolan, T. W. Kensler, G. H. Posner, *Bioorg. Med. Chem.* **2009**, *17*, 5627. <https://doi.org/10.1016/j.bmc.2009.06.033>
- [8] J. N. Dominguez, C. Leon, J. Rodrigues, N. G. de Dominguez, J. Gut, P. J. Rosenthal, *Eur. J. Med. Chem.* **2009**, *44*, 1457. <https://doi.org/10.1016/j.ejmech.2008.09.044>
- [9] D. C. Meadows, T. Sanchez, N. Neamati, T. W. North, J. Gervay-Hague, *Bioorg. Med. Chem.* **2007**, *15*, 1127. <https://doi.org/10.1016/j.bmc.2006.10.017>
- [10] Z. Li, R. Yazaki, T. Ohshima, *Org. Lett.* **2016**, *18*, 3350. <https://doi.org/10.1021/acs.orglett.6b01464>
- [11] Y. Zhu, Y. Ni, V. A. Soloshonok, J. Han, Y. Pan, *J. Fluorine Chem.* **2019**, *219*, 32. <https://doi.org/10.1016/j.jfluchem.2018.12.009>
- [12] A. A. Hassan, Y. R. Ibrahim, A. M. Shawky, *J. Sulfur Chem.* **2007**, *28*, 211. <https://doi.org/10.1080/17415990701230596>
- [13] A. A. Hassan, N. K. Mohamed, A. M. Shawky, D. Döpp, *ARKIVOC* **2003**, *i*, 118. <https://doi.org/10.3998/ark.5550190.0004.114>
- [14] A. A. Hassan, F. F. Abdel-Latif, A. M. N. El-Din, M. Abdel-Aziz, S. M. Mostafa, S. Bräse, *J. Heterocycl. Chem.* **2011**, *48*, 1050. <https://doi.org/10.1002/jhet.687>
- [15] A. A. Hassan, Y. R. Ibrahim, A. M. Shawky, D. Döpp, *J. Heterocycl. Chem.* **2006**, *43*, 849. <https://doi.org/10.1002/jhet.5570430406>
- [16] A. Pasternak, S. Dong, J. D. Scott, H. Tang, Z. Zhao, D. Yang, X. Gu, J. Jiang, L. Xiao, *WO 2019018186 A1 20190124*, **2019**.
- [17] United States (12) Patent Application, *US0128660A1*, **2006**.
- [18] W. Ma, Y. Xie, X. Liao, J. Huang, W. Lin, Z. Long, *AU 2018100066, A4 20180215*, **2018**.
- [19] A. A. Aly, A. A. Hassan, N. K. Mohamed, K. M. El-Shaieb, M. M. Makhoulf, S. Bräse, M. Nieger, *Res. Chem. Intermed.* **2019**, *45*, 613. <https://doi.org/10.1007/s11164-018-3633-4>
- [20] E. M. El-Sheref, A. A. Aly, A.-F. E. Mourad, A. B. Brown, S. Bräse, M. E. M. Bakheet, *Chem. Pap.* **2018**, *72*, 181. <https://doi.org/10.1007/s11696-017-0269-6>
- [21] A. A. Aly, E. M. El-Sheref, A.-F. E. Mourad, A. B. Brown, S. Bräse, M. E. M. Bakheet, M. Nieger, *Monatsh. Chem.* **2018**, *149*, 635. <https://doi.org/10.1007/s00706-017-0278-6>
- [22] A. A. Aly, E. M. El-Sheref, A.-F. E. Mourad, M. E. M. Bakheet, S. Bräse, M. Nieger, *Chem. Pap.* **2019**, *73*, 27. <https://doi.org/10.1007/s11696-018-0561-0>
- [23] A. A. Aly, M. Ramadan, A. A. M. El-Reedy, *J. Heterocycl. Chem.* **2019**, *56*, 642. <https://doi.org/10.1002/jhet.3442>
- [24] A. A. Aly, E. M. El-Sheref, M. E. M. Bakheet, A.-F. E. Mourad, S. Bräse, M. A. A. Ibrahim, M. Nieger, B. K. Garvalov, K. N. Dalby, T. S. Kaoud, *Bioorg. Chem.* **2019**, *82*, 290. <https://doi.org/10.1016/j.bioorg.2018.10.044>
- [25] A. A. Aly, E. M. El-Sheref, M. E. M. Bakheet, A.-F. E. Mourad, A. B. Brown, S. Bräse, M. Nieger, M. A. A. Ibrahim, *Bioorg. Chem.* **2018**, *81*, 700. <https://doi.org/10.1016/j.bioorg.2018.09.017>
- [26] A. A. Aly, E. M. El-Sheref, A.-F. E. Mourad, M. E. M. Bakheet, S. Bräse, *Mol. Divers.* **2020**, *24*, 477. <https://doi.org/10.1007/s11030-019-09952-5>
- [27] M. A. I. Elbastawesy, A. A. Aly, M. Ramadan, Y. A. M. M. Elshairer, B. G. M. Youssif, A. B. Brown, G. E.-D. A. Abu-Rahma, *Bioorg. Chem.* **2019**, *90*, 103045. <https://doi.org/10.1016/j.bioorg.2019.103045>
- [28] G. Gilman, L. S. Goodman, *The Pharmacological Basis of Therapeutics*, 5th ed., Macmillan, New York **1985**.
- [29] P. Zimmet, K. G. Alberti, J. Shaw, *Nature* **2001**, *414*, 782. <https://doi.org/10.1038/414782a>
- [30] R. A. Defronzo, R. C. Bonadonna, E. Ferrannini, *Diabetes Care* **1992**, *15*, 318. <https://doi.org/10.2337/diacare.15.3.318>
- [31] M. Rendell, *Drugs* **2004**, *64*, 1339. <https://doi.org/10.2165/00003495-200464120-00006>
- [32] M. Kumar, D. Verma, *Pharmacologyonline* **2011**, *2*, 307.
- [33] S. Mihailova, A. Tsvetkova, A. Todorova, *Int. Arch. Integr. Med* **2015**, *2*, 223.
- [34] B. D. Prendergast, *Clin. Pharm.* **1984**, *3*, 473.
- [35] S. Del Prato, N. Pulizzi, *Metabolism* **2006**, *55*, S20. <https://doi.org/10.1016/j.metabol.2006.02.003>
- [36] G. Shammii, K. R. Jitendra, R. K. Narang, K. S. Rajesh, *Int. J. Pharm. Pharm. Sci.* **2010**, *2*, 1.
- [37] N. Hosseinzadeh, S. Seraj, M. E. Bakhshi-Dezffoli, M. Hasani, M. Khoshneviszadeh, S. Fallah-Bonekohal, M. Abdollahi, A. Foroumadi, A. Shafiee, *Iran. J. Pharm. Res.* **2013**, *12*, 325.
- [38] H. M. Faidallah, K. A. Khan, *J. Fluorine Chem.* **2012**, *142*, 96. <https://doi.org/10.1016/j.jfluchem.2012.06.032>
- [39] G. Mariappan, B. P. Saha, S. Datta, D. Kumar, P. K. Haldar, *J. Chem. Sci.* **2011**, *123*, 335.
- [40] L. Mahmoodnia, E. Aghadavod, S. Beigrezaei, M. Rafieian-Kopaei, *J. Renal Inj. Prev.* **2017**, *6*, 153. <https://doi.org/10.15171/jrip.2017.30>
- [41] S. M. Fernandes, P. M. Cordeiro, M. Watanabe, C. D. da Fonseca, M. F. F. Vattimo, *Arch. Endocrinol. Metab.* **2016**, *60*, 443. <https://doi.org/10.1590/2359-3997000000188>
- [42] C. C. Beals, J. Bullock, E. R. Jauregui, W. N. Duran, *Microvasc. Res.* **1993**, *45*, 11. <https://doi.org/10.1006/mvres.1993.1002>
- [43] J. Ditzel, *Diabetes* **1968**, *17*, 388. <https://doi.org/10.2337/diab.17.6.388>
- [44] P. E. Jennings, A. H. Barnett, *Diabet. Med.* **1988**, *5*, 111. <https://doi.org/10.1111/j.1464-5491.1988.tb00955.x>
- [45] S. A. Wohaieb, D. V. Godin, *Diabetes* **1987**, *36*, 1014. <https://doi.org/10.2337/diab.36.9.1014>

- [46] A. J. Sinclair, *Diabetes Rev.* **1993**, *2*, 7.
- [47] A. A. Hassan, A.-F. E. Mourad, K. M. El-Shaieb, A. F. Abou-Zied, *Molecules* **2005**, *10*, 822. <https://doi.org/10.3390/10070822>
- [48] H. O. Fong, W. R. Hardstaff, D. G. Kay, R. F. Langler, R. H. Morse, D.-N. Sandoval, *Can. J. Chem.* **1979**, *57*, 1206.
- [49] C. Njera, M. Yus, *Tetrahedron* **1990**, *55*, 10547. [https://doi.org/10.1016/S0040-4020\(99\)00600-6](https://doi.org/10.1016/S0040-4020(99)00600-6)
- [50] P. A. Rowe, M. L. Campbell-Thompson, D. A. Schatz, M. A. Atkinson, *Semin. Immunopathol.* **2011**, *33*, 29. <https://doi.org/10.1007/s00281-010-0208-x>.
- [51] D. O. Adeyemi, O. A. Komolafe, O. S. Adewole, E. M. Obuotor, A. A. Abiodun, T. K. Adenowo, *Folia Morphol.* **2010**, *69*, 92.
- [52] E. Larger, M. F. Philippe, L. Barbot-Trystram, A. Radu, M. Rotariu, E. Nobécourt, C. Boitard, *Diabet. Med.* **2012**, *29*, 1047. <https://doi.org/10.1111/j.1464-5491.2012.03597.x>
- [53] N. Li, J.-X. Wu, D. Ding, J. Cheng, N. Gao, L. Chen, *Cell* **2017**, *168*, 101. <https://doi.org/10.1016/j.cell.2016.12.02>
- [54] B. Stanovnik, M. Tisler, *J. Org. Chem.* **1960**, *25*, 2234. <https://doi.org/10.1021/jo01082a613>
- [55] B. K. Çavusoglu, B. N. Sağlık, D. Osmaniye, S. Levent, U. A. Çevik, A. B. Karaduman, Y. Özkay, Z. A. Kaplancık, *Molecules* **2018**, *23*, 60. <https://doi.org/10.3390/molecules23010060>
- [56] M. Paranjpe, *Indian J. Chem.* **1969**, *7*, 186.
- [57] I. V. Nikolaeva, A. A. Tsurkan, I. B. Levshin, K. A. V., Yunov, A. I. Ginak, *Zh. Prakt. Khim. (Leningrad)* **1985**, *58*, 1189. Chem. Abstr. 1985, 103, 177952h.
- [58] R. Yella, N. Khatun, S. K. Rout, B. K. Patel, *Org. Biomol. Chem.* **2011**, *9*, 3235. <https://doi.org/10.1039/C0OB01007C>
- [59] G. M. Sheldrick, *Acta Crystallogr.* **2015**, *A71(1)*, 3. <https://doi.org/10.1107/S2053273314026370>
- [60] G. M. Sheldrick, *Acta Crystallogr.* **2015**, *C71(1)*, 3. <https://doi.org/10.1107/S2053229614024218>
- [61] S. Parson, H. D. Flack, T. Wagner, *Acta Crystallogr.* **2013**, *B69*, 249. <https://doi.org/10.1107/S2052519213010014>
- [62] A. R. Cowley, J. R. Dilworth, P. S. Donnelly, A. D. Gee, J. M. Heslop, *Dalton Trans.* **2004**, 2404. <https://doi.org/10.1039/b406429a>
- [63] A. W. Maverick, J. K. Cherutoi, F. R. Fronczek, CCDC 808735: *Experimental Crystal Structure Determination*, Cambridge Crystallographic Data Centre, Cambridge, United Kingdom **2014**. <https://doi.org/10.5517/ccw4k7s>
- [64] B. Jayaprasad, P. Sharavanan, R. Sivaraj, *Beni-Suef Univ. J. Basic Appl. Sci.* **2016**, *5*, 61. <https://doi.org/10.1016/j.bjbas.2016.01.004>
- [65] J. N. Sangshetti, D. K. Lokwani, A. P. Sarkate, D. B. Shinde, *Chem. Biol. Drug Des.* **2011**, *78*, 800. <https://doi.org/10.1111/j.1747-0285.2011.01178.x>
- [66] J. A. Buege, S. D. Aust, S. Fleischer, L. Packer, *Methods Enzymol.* **1978**, *52*, 302.
- [67] M. S. Moron, J. W. Depierre, B. Mannervik, *Biochim. Biophys. Acta* **1979**, *582*, 67. [https://doi.org/10.1016/0304-4165\(79\)90289-7](https://doi.org/10.1016/0304-4165(79)90289-7)
- [68] S. Côté, *Immunohistochemistry* **1993**, *II*, 148.
- [69] E. A. Elbassuoni, S. M. Abdel Hafez, *Cell Stress Chaperones* **2019**, *24*, 567. <https://doi.org/10.1007/s12192-019-00988-y>
- [70] N. Süleymanoğlu, R. Ustabaş, S. Direkel, Y. B. Alpaslan, Y. Ünver, *J. Mol. Struct.* **2017**, *1150*, 82. <https://doi.org/10.1016/j.molstruc.2017.08.075>

SUPPORTING INFORMATION

Additional Supporting Information may be found online in the supporting information tab for this article.

How to cite this article: Aly AA, Hassan AA, Makhlof MM, et al. Design and synthesis of hydrazinecarbothioamide sulfones as potential antihyperglycemic agents. *Arch Pharm.* 2021;354: e2000336. <https://doi.org/10.1002/ardp.202000336>